



Cite this: *Phys. Chem. Chem. Phys.*,
2015, 17, 11740

A density functional theory based study of the electron transfer reaction at the cathode–electrolyte interface in lithium–air batteries†

Saeed Kazemiabnavi,‡ Prashanta Dutta‡ and Soumik Banerjee*‡

The unique properties of ionic liquids such as a relatively wide electrochemical stability window and very low vapor pressure have made them promising candidates as electrolytes for improving the cyclic performance of lithium–air batteries. The local current density, which is an important parameter in determining the performance of lithium–air batteries, is a function of the rate constant of the electron transfer reactions at the surface of the cathode. In this study, a novel method based on Marcus theory is presented to investigate the effect of varying the length of the alkyl side chain of model imidazolium based cations and the operating temperature on the rates of electron transfer reactions at the cathode. The necessary free energies of all the species involved in the multi-step reduction of oxygen into the peroxide ion were calculated using density functional theory (DFT). Our results indicate that the magnitude of the Gibbs free energy for the reduction of oxygen into the superoxide ion and also for the reduction of superoxide into the peroxide ion increases with an increase in the static dielectric constant of the ionic liquid. This trend in turn corresponds to the decrease in the length of the alkyl side chain of the ionic liquid cation. Furthermore, the change in Gibbs free energy decreases with increase in the operating temperature. The inner-sphere reorganization energies were evaluated using Nelsen's four point method. The total reorganization energies of all reduction reactions increase with decrease in the length of the alkyl side chain and increase in the operating temperature. Finally, the rate constants of the electron transfer reaction involved in the reduction of oxygen were calculated. The logarithm of the reaction rate constants decreases with increase in the static dielectric constant and increases with increase in the operating temperature. Our results provide fundamental insight into the kinetics and thermodynamics of the electron transfer reactions at the cathode that will help in the identification of appropriate electrolytes for enhanced performance of lithium–air batteries.

Received 31st December 2014,
Accepted 31st March 2015

DOI: 10.1039/c4cp06121g

www.rsc.org/pccp

Introduction

The energy density of state-of-the-art Li-ion cells falls short of the target of 1700 W h kg⁻¹.¹ Therefore, the scientific community has shown increasing interest in exploring coupled electrochemical reactions with significantly higher theoretical gravimetric energy densities compared to Li-ion cells that comprise two intercalation electrodes.² Li–air batteries, where the lithium metal anode is electrochemically coupled with oxygen, exhibit extremely high theoretical energy density.³ These batteries have potential applications in long-range electric vehicles, where gravimetric energy density, volumetric energy density and safety are key factors that

define performance.^{1,4} Additionally, Li–air batteries can be very beneficial in powering myriad consumer electronic devices as well as remote sensors.²

Due to the high chemical reactivity of metallic lithium,⁵ safety is one of the primary concerns in all the above-mentioned applications of lithium batteries.^{6,7} Lithium metal is highly reactive in the presence of polar protic and aprotic organic solvents, commonly used as electrolytes in lithium batteries, and can lead to electrode–electrolyte side reactions.⁸ Furthermore, the typically high vapor pressure of organic solvents leads to increased flammability of the battery. Therefore, the use of Li–air batteries with organic liquid electrolytes in aerospace and automobile industries is contingent upon finding novel electrolytes that lead to increased safety standards.⁹ In addition to reduced flammability, the properties of an ideal electrolyte need to be tailored to enhance the performance when used in Li–air batteries. In particular, the electrochemical stability and other physicochemical properties of the electrolyte, such as static and

School of Mechanical and Materials Engineering, Washington State University,
Pullman, WA, 99164-2920, USA. E-mail: soumik.banerjee@wsu.edu;
Tel: +1 509 3350294

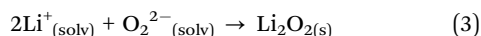
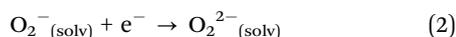
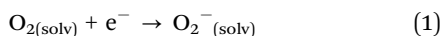
† Electronic supplementary information (ESI) available. See DOI: 10.1039/c4cp06121g

‡ These authors contributed equally.

optical dielectric constants, ionic conductivity, and ability to dissolve various chemical species generated during the electrochemical reactions, can significantly impact the cyclic performance of Li-air batteries.⁴ Room temperature ionic liquids (RTILs), which have high electrical conductivity, wide electrochemical stability window as well as low vapor pressure, are safer alternatives to conventional liquid electrolytes used in lithium batteries.^{10–12} A qualitative comparison of ionic liquids with organic solvents shows that ionic liquids also have higher thermal stability and tunable solvating ability.¹³

Room temperature ionic liquids are salts comprising cations that are typically based on cyclic amines, both aromatic (pyridinium, imidazolium) and saturated (piperidinium, pyrrolidinium). Combining these cations with both inorganic and organic anions such as $[\text{BF}_4]^-$, $[\text{PF}_6]^-$, $[\text{N}(\text{CF}_3\text{SO}_2)_2]^-$ and $[\text{CF}_3\text{CONCF}_3\text{SO}_2]^-$, results in various ionic liquids with a wide variety of tunable physicochemical and electrochemical properties.¹¹ It is also possible to tune these properties by changing the chemical structure of these ions. The tunability of ionic liquids provides the opportunity to synthesize specific cations with desired properties such as to use them as electrolytes for lithium batteries with enhanced performance.

The local current density is one of the crucial factors governing the performance of lithium-air batteries. Using the framework of the Butler-Volmer equation, the current density at the cathode is expressed as a function of the electron transfer rate constant for the electrochemical reaction at the electrode-electrolyte interface.^{14,15} During the discharge cycle of Li-air batteries, solvated oxygen gets reduced at the cathode producing the peroxide ion, which forms lithium peroxide as the final discharge product.¹⁶ The overall reaction comprises the following steps:



The reverse reactions occur during the charge cycle and the peroxide ion gets oxidized to oxygen. Each electrochemical reduction reaction occurs in a single step.^{1,16}

The oxygen reduction reaction (ORR) mechanism in aprotic organic electrolytes on a glassy carbon electrode was recently studied by Laoire *et al.*^{17,18} using cyclic voltammetry and a rotating disc electrode technique. The results indicated that lithium superoxide (LiO_2) is formed initially and then converted to lithium peroxide (Li_2O_2) either by disproportionation reaction or by further reduction. However, computational studies have indicated that lithium superoxide is very unstable at room temperature at less than 1 atm oxygen pressure.^{19,20} Although other reaction products such as Li_2O and Li_2CO_3 have been observed in the experiment, *ex situ* examination of the cathode products from discharged Li/ O_2 cells using Raman spectroscopy²¹ as well as oxygen consumption stoichiometry in the discharge process,²² have confirmed that Li_2O_2 is the major ORR product.

In previous studies, we presented a method for calculating the electron transfer rate constant of the oxidation of lithium metal at the anode of a lithium-air battery and investigated the

effect of the static dielectric constant of the electrolyte on the reaction rate constants.^{23,24} However, the literature lacks detailed studies that describe the influence of the molecular structure of liquid electrolytes on the kinetics of the electrochemical reactions at the cathode, which has a crucial impact on the performance of batteries. In an effort to investigate the effect of the specific molecular structure of ionic liquid based electrolytes on the thermodynamics and kinetics of the cathodic reactions, in the present study, we obtained a trend for the variation of the Gibbs free energy change and the electron transfer rate constants of the cathodic reactions as a function of the operating temperature and the dielectric constant of the electrolyte. We calculated the electron transfer rate constant for the multi-step reduction of oxygen on the porous carbon cathode in the presence of ionic liquids with varying structures of the cation and at various operating temperatures.

In particular, in this study, 1-alkyl-3-methylimidazolium bis(trifluoromethanesulfonyl)-amide ($\text{C}_n\text{MIM}^+\text{TFSI}^-$) ionic liquids with varying number of carbon atoms in the alkyl side chain, n , were chosen as the model electrolytes. This ionic liquid was selected due to the relatively low viscosity, wide electrochemical stability window and higher ionic conductivity of imidazolium based cations compared to other ionic liquids.^{11,25–28} Additionally, the desired physical properties of these ionic liquids that are required as input to the *ab initio* calculations, such as static and optical dielectric constants have been characterized in several studies^{25,29} and are readily available. The commonly used TFSI^- anion was chosen due to its wide electrochemical stability window and low viscosity when coupled with imidazolium based cations compared to other anions such as BF_4^- and PF_6^- .^{26,30–38} Fig. 1 shows the chemical structures of a sample imidazolium cation for $n = 3$ and the TFSI^- anion.

Transition State Theory (TST)³⁹ and other theories, based in whole or in part on the fundamental assumptions of TST, as well as some quantum mechanical generalization of these assumptions, are typically used to calculate the chemical reaction rates.^{40–42} However, these theories cannot be applied to electron transfer reactions since describing the transition state in this type of reactions is not practically possible. The Marcus theory has been widely used to evaluate the reaction rate constants for several electron transfer reactions between separated donor and acceptor species and show excellent agreement with experimental results.⁴³ In the present study, the Marcus theory⁴³ formulation was employed to calculate the electron transfer reaction rate constants

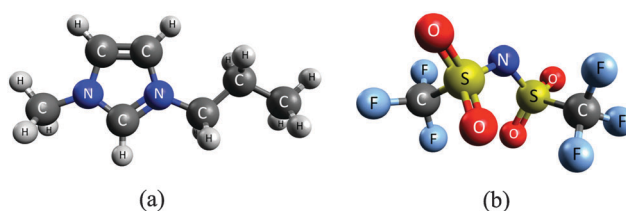
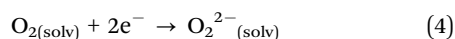


Fig. 1 The chemical structures of the model ionic liquid (a) 1-propyl-3-methylimidazolium (C_3MIM^+) cation and (b) bis(trifluoromethanesulfonyl)-amide (TFSI^-) anion are shown.

using relevant thermodynamic parameters. The Gibbs free energy, inner- and outer-sphere reorganization energies and the electronic coupling energy were calculated to evaluate the rate constant based on Marcus theory. The solvation energy of separated ions and molecules was calculated to determine the effect of solvent on the thermodynamic driving force and the reaction rate. Finally, the aforementioned thermodynamic parameters were calculated for a range of temperatures that are typically encountered during the operation of Li-air batteries in order to investigate the effect of temperature on the reaction rates at the cathode.

Methodology

The main goal of the present study is to investigate the effect of the structure of the ionic liquid's cation as well as the operating temperature on the electron transfer reaction rates at the cathode. The reduction reaction of solvated oxygen at the cathode, due to electron transfer, can be represented as:



In the framework of Marcus theory, the reaction rate is a function of the Gibbs free energy for the reaction and a kinetic pre-factor:

$$k_{\text{et}} = \frac{2\pi}{\hbar} |V_{\text{RP}}|^2 \frac{1}{\sqrt{4\pi\lambda k_{\text{B}} T}} \exp\left(-\frac{(\lambda + \Delta G^\circ)^2}{4\lambda k_{\text{B}} T}\right) \quad (5)$$

In this equation k_{et} is the rate constant for electron transfer, $|V_{\text{RP}}|$ is the electronic coupling energy between the initial and final states, \hbar is the reduced Planck's constant $h/2\pi$, λ is the total reorganization energy, ΔG° is the total Gibbs free energy change for the electron transfer reaction, k_{B} is the Boltzmann constant and T is the absolute temperature.

In order to calculate the Gibbs free energy of this reaction, the overall reduction process of oxygen at the cathode is assumed to occur in two consecutive steps as shown in eqn (1) and (2). The first reaction is the reduction of neutral oxygen to superoxide followed by the reduction of the superoxide ion into peroxide. All these species are solvated in the electrolyte. The Gibbs free energy of the complete reaction can be calculated by adding the corresponding free energies of the constituent reactions:

$$\Delta G^\circ = \Delta G_1^\circ + \Delta G_2^\circ \quad (6)$$

where, ΔG° is the Gibbs free energy of the overall reaction, ΔG_1° and ΔG_2° are the Gibbs free energies of the reduction of oxygen into superoxide and the reduction of superoxide into peroxide respectively. In order to calculate the Gibbs free energy of the first and second reduction reactions in the solvated phase, the optimized structures of each species was determined using density functional theory followed by a frequency analysis and single point energy calculations in the solution phase. These calculations provided the Gibbs free energy of individual reactants and products. The difference between the free energies of reactant and products was then used to evaluate the Gibbs free energy of each reduction reaction:

$$\Delta G_1^\circ = G^\circ(\text{O}_2^-) - G^\circ(\text{O}_2) \quad (7)$$

$$\Delta G_2^\circ = G^\circ(\text{O}_2^{2-}) - G^\circ(\text{O}_2^-) \quad (8)$$

where, $G^\circ(\text{O}_2)$, $G^\circ(\text{O}_2^-)$ and $G^\circ(\text{O}_2^{2-})$ are the Gibbs free energies of the neutral oxygen molecule, superoxide and peroxide ions respectively. In addition to its dependence on the Gibbs free energy, the electron transfer rate constant is also a function of the inner- and outer-sphere reorganization energies in the framework of Marcus theory, as shown in eqn (5). The total reorganization energy is given by the summation of the inner-sphere and outer-sphere reorganization energies, $\lambda = \lambda_{\text{in}} + \lambda_{\text{out}}$, which are independent parameters.

Nelsen's four point method,⁴⁴ which is one of the most prevalent methods used to calculate the inner-sphere reorganization energy by separating oxidants and reductants, is expressed as:⁴⁵

$$\lambda_{\text{in}} = [E(\text{D}^+|\text{D}) - E(\text{D}^+|\text{D}^+)] + [E(\text{A}^-|\text{A}) - E(\text{A}^-|\text{A}^-)] \quad (9)$$

where $E(\text{a}|\text{b})$ is the energy of state "a" calculated at the equilibrium structure of state "b", D designates donor species, A designates the acceptor species and +/- superscript designates the charge on the species. The model system that was used to calculate the inner-sphere reorganization energy is shown in Fig. 2. The system consists of 36 carbon atoms in the form of two parallel graphite layers each with 18 carbon atoms. On the top of these two layers one oxygen molecule is placed 3.36 Å above the surface. A theoretical study of oxygen adsorption on graphite by Sorescu *et al.*⁴⁶ showed that the physisorbed oxygen molecule that is constrained to lie parallel to the graphite surface is located 3.36 Å above the surface and retains its spin triplet character. Moreover, chemisorbed triplet oxygen molecules that are chemically bound to the underlying C-C bond were also characterized. Chemisorbed oxygen molecules, however, have a much longer O-O distance (2.03 Å) and are in fact two weakly interacting oxygen atoms that are strongly bound to the carbon atoms on the surface.

The oxygen molecules on top of the graphite layer act as the acceptor and the carbon atoms in the graphitic cathode, which have an extra negative charge, act as the donor. The porous carbon cathode is modeled as a graphitic layer. The lattice structure of the parallel graphitic layers and the corresponding lattice parameters in the cathode side were assumed to remain constant during the electron transfer reaction and only the oxygen or superoxide molecules above the layer are reduced during the reactions resulting in a change in their structure.

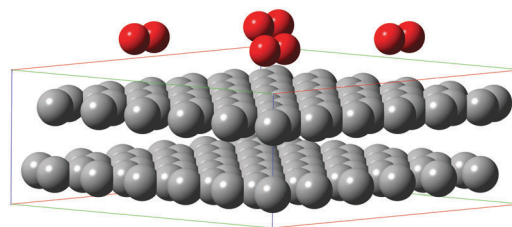


Fig. 2 The configuration of the model system used in DFT calculation for inner-sphere reorganization energy is shown. While the actual modeled system comprises 36 carbon atoms as the donor species, a larger periodic domain has been shown for the purpose of illustration. Red: oxygen or superoxide molecule. Gray: carbon atom.

Accordingly, since D^+ and D have the same lattice structures, $E(D^+|D)$ is assumed to be equal to $E(D^+|D^+)$. Therefore the contribution of the change in the energy states of donor species to inner-sphere reorganization energy is negligible. Hence, the abridged expressions for inner-sphere reorganization energies for the reduction of oxygen and superoxide at the cathode, $\lambda_{in,1}$ and $\lambda_{in,2}$, and their corresponding backward reactions, $\lambda_{in,\bar{1}}$ and $\lambda_{in,\bar{2}}$, are given as:

$$\lambda_{in,1} = [E(O_2^-|O_2) - E(O_2^-|O_2^-)] \quad (10a)$$

$$\lambda_{in,\bar{1}} = [E(O_2|O_2^-) - E(O_2|O_2)] \quad (10b)$$

$$\lambda_{in,2} = [E(O_2^{2-}|O_2^-) - E(O_2^{2-}|O_2^{2-})] \quad (11a)$$

$$\lambda_{in,\bar{2}} = [E(O_2^-|O_2^{2-}) - E(O_2^-|O_2^-)] \quad (11b)$$

In these equations, the terms $E(O_2^-|O_2)$ and $E(O_2^{2-}|O_2^{2-})$ represent the energies of superoxide and peroxide ions in the solvated phase respectively. Based on the physical meaning of reorganization energy, the above equations provide the value of the energy which is needed to “reorganize” the system from its initial to final coordinates after the charge is transferred for the two-step reduction of oxygen into the peroxide ion.

The classical electrostatics model based on Marcus theory⁴³ was implemented to calculate the outer-sphere reorganization energy:

$$\lambda_{out} = \frac{\Delta e^2 N_A}{8\pi\epsilon_0} \left(\frac{1}{r} - \frac{1}{R_e} \right) \left(\frac{1}{\epsilon_{op}} - \frac{1}{\epsilon_s} \right) \quad (12)$$

where, r is the ionic radius, R_e is twice the distance from the surface of the electrode at which the electron transfer reaction takes place, ϵ_s and ϵ_{op} are, the static and high frequency optical dielectric constants of the solvent, Δe is the amount of charge transferred, N_A is Avogadro's number and ϵ_0 is the permittivity of vacuum. We assumed that the electron transfer reactions take place when the acceptor molecules (oxygen or superoxide) are located at 3.36 Å above the surface of the graphite layers.⁴⁶ Therefore, R_e will be equal to 6.72 Å.

The electronic coupling energy was calculated using the method of Corresponding Orbital Transformation after obtaining the initial and final wave functions, Ψ_a and Ψ_b .^{47,48}

$$V_{a,b} = (1 - S_{a,b}^2)^{-1} \left| H_{a,b} - \frac{1}{2} S_{a,b} (H_{a,a} + H_{b,b}) \right| \quad (13)$$

where, $S_{a,b} = \langle \Psi_a | \Psi_b \rangle$ is the reactant-product overlap, H is the total electronic Hamiltonian, excluding nuclear kinetic energy and nuclear repulsion terms of the system, $H_{a,b} = \langle \Psi_a | H | \Psi_b \rangle$ is the total interaction energy, also referred to as “electronic coupling matrix element”, and $H_{a,a} = \langle \Psi_a | H | \Psi_a \rangle$ is the electronic energy of reactants or products. Usually $V_{a,b}$ is very weak in electron transfer reactions. Based on the required parameters including electronic coupling energy, reorganization energies and the Gibbs free energies of the reactions, Marcus theory was employed to calculate the electron transfer rate constants of both reduction reactions, in the forward and backward directions.

Finally, in order to investigate the effect of temperature on the reaction rates, the Gibbs free energy of each species was

calculated at temperatures ranging from -15 °C to 100 °C in $[C_2MIM]^+ [TFSI]^-$ as the solvent and the corresponding rate constants of each reduction reaction in both forward and backward directions were calculated. The Gibbs free energy of a molecule can be calculated using eqn (14):

$$G = H - TS \quad (14)$$

where T is the absolute temperature, G is the Gibbs free energy, H is the enthalpy and S is the total entropy of a molecule. The enthalpy of a molecule, H , at each temperature is the sum of the total internal energy of the molecule, E , and the thermal correction to the enthalpy, $H_{correction}$:

$$G = (E + H_{correction}) - TS \quad (15)$$

The thermal correction to the enthalpy as well as the total entropy of each species can be obtained from a frequency calculation. The solvation energy and the electronic coupling energy are invariant with the temperature. Using the calculated Gibbs free energies, the required thermodynamic parameters for Marcus theory including the Gibbs free energy change and the reorganization energy of each reduction reaction were calculated and utilized to evaluate the rate constant of each reaction in both forward and backward directions.

In this study, all optimization, energy and frequency calculations were done using Density Functional Theory (DFT) with the Becke, three-parameter, Lee–Yang–Parr^{49,50} (B3LYP) exchange–correlation functional and 6-311++G** (ref. 51) as the basis set, which is a Valence Triple Zeta basis set with polarization and diffuse functions on all atoms (VTZPD). The zero-point energies of the species involved in the oxygen reduction reaction are provided in Table S1 in the ESI.† To further support the results, a cross checking calculation using MP2 level of theory was performed (Table S2, ESI†) which shows only 0.2% difference in the total energy of the oxygen molecules. All calculations were done using the NWChem 6.1 computational chemistry software package.⁵²

In order to account for the dielectric screening in solvents, the Conductor-like Screening Model⁵³ (also known as the COSMO solvation model) was implemented to study the effect of solvent on reaction rates. The key inputs to this model are the dielectric constant of the solvent as well as the radii of solvated species and solvent molecules. For all calculations, the oxygen, superoxide and peroxide species are only surrounded by the C_nMIM^+ cations, with varying radii as the number of carbon atoms in the alkyl side chain changes. Therefore, the dielectric constant is not the only parameter that determines the solvation energy since the solvent radius varies for different ionic liquids. Fig. 3 shows the variation of the static dielectric constant²⁵ and the radius of the imidazolium based cation⁵⁴ that were chosen for this study. Increasing the number of carbon atoms in the alkyl side chain of the imidazolium cation causes an expected increase in the solvent radius and decrease in the static dielectric constant of the imidazolium cation based ionic liquid.

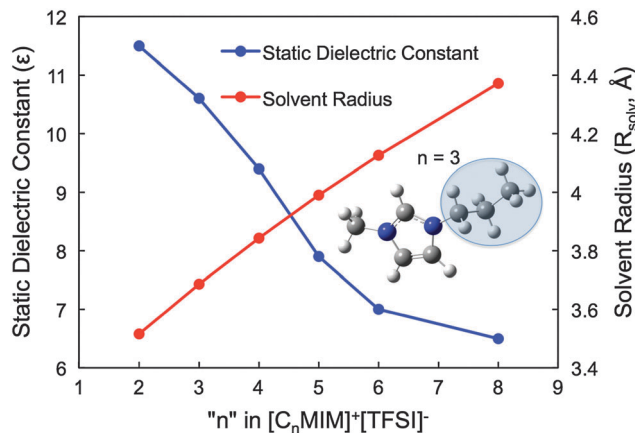


Fig. 3 Static dielectric constant, ϵ , and solvent radius, R_{solv} (Å), of some imidazolium based ionic liquids with the TFSI⁻ anion are shown.^{25,54} The difference in the number of carbons in the alkyl side chain results in different values of the static dielectric constant. The static dielectric constant decreases as the length of the side chain, and therefore the solvent radius, increases.

Results and discussion

In order to calculate the Gibbs free energy change for each reaction and their corresponding reorganization energies based on eqn (7) to (11), it is necessary to determine the Gibbs free energy of each species first. Nelson's four-point method, described in eqn (9)–(11), further requires the evaluation of Gibbs free energy of the oxygen molecule, the superoxide ion and the peroxide ion in the optimized structure of a different molecule or ion. Fig. 4–6 present these Gibbs free energies for the oxygen molecule, the superoxide ion and the peroxide ion respectively. The energies were calculated for the specific electronic charge on the optimized structure of the respective chemical species as well as for excess or diminished charges on identical optimized structure, as required for applying Nelson's four-point method.

Fig. 4 shows the variation of the Gibbs free energy of an oxygen molecule in both neutral and negatively charged states, for optimized structure that corresponds to neutral oxygen, with the dielectric constant of the solvent. The solvation energies of both neutral and negatively charged oxygen are negative. Therefore, increasing the dielectric constant, which results in an increase in the magnitude of the solvation energy, causes the Gibbs free energy of neutral and negatively charged oxygen in the solvated phase to be more negative. However, the effect of increase in the magnitude of the solvation energy of neutral oxygen cannot be seen in this plot since the maximum difference in the Gibbs free energy of neutral oxygen in different ionic liquids is 6.5 J mol^{-1} which is only $1.6 \times 10^{-6}\%$ of its average value.

The Gibbs free energy of a superoxide molecule with 0, -1 and -2 electronic charges is shown in Fig. 5. The optimized structures for all charges correspond to a superoxide ion with -1 charge. As can be seen from the graph, the Gibbs free energy of a superoxide ion with charges of -1 and $-2 e$ is more negative in solvents with higher dielectric constant. This trend

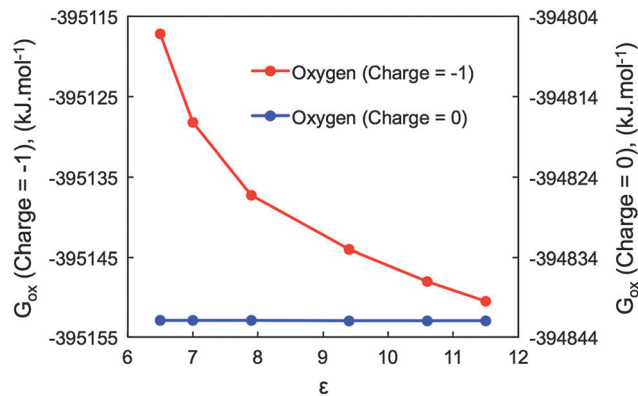


Fig. 4 The variation of the Gibbs free energy of neutral and negatively charged oxygen, G_{ox} , with the dielectric constant of the solvent, ϵ , is shown. The optimized structure corresponds to that of the neutral oxygen molecule. The Gibbs free energy of neutral oxygen remains almost constant with varying dielectric constant.

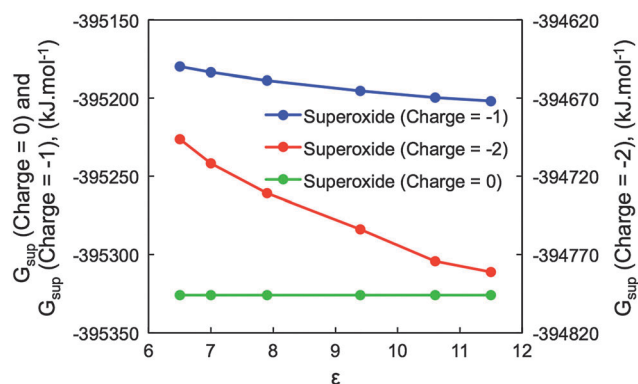


Fig. 5 The Gibbs free energy of neutral, $-1 e$ and $-2 e$ charged superoxide structure, G_{sup} , are shown as a function of the static dielectric constant of the solvent. The optimized structure corresponds to that of the superoxide ion with a negative charge of $-1 e$. The Gibbs free energy of neutral superoxide is almost independent of the dielectric constant.

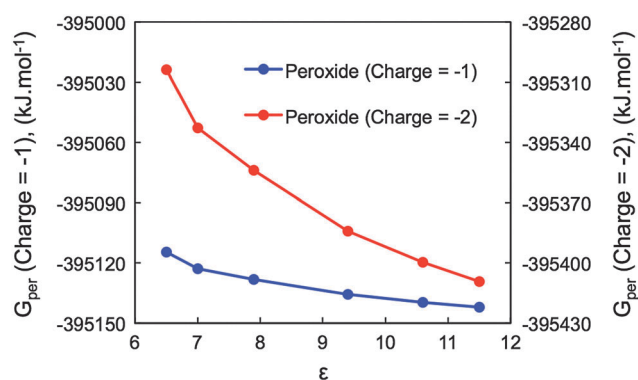


Fig. 6 The variation of the Gibbs free energy of the $-1 e$ and $-2 e$ charged peroxide ion, G_{per} , with the static dielectric constant of the solvent is presented. The optimized structure corresponds to that of the peroxide ion with a negative charge of $-2 e$ charge.

is expected since the solvation energies of these species are negative. Fig. 5 indicates that the rate of decrease in the solvation energy of the superoxide ion with a charge of $-2 e$

with the dielectric constant is higher than that of a superoxide ion with a charge of $-1 e$. This trend is caused by the greater electrostatic charge on -2 charged species compared to that of -1 and is expected from the COSMO solvation model.⁵³ These results also agree with the study conducted by Tjong and Zhou on the dependence of electrostatic solvation energy of charged species on the dielectric constant of solvent.⁵⁵ The maximum difference in the Gibbs free energy of neutral superoxide in different ionic liquids is 180.5 J mol^{-1} which is only $4.6 \times 10^{-5}\%$ of its average value and therefore remains almost constant.

The Gibbs free energies of peroxide with charges of -1 and $-2 e$ are presented in Fig. 6. The solvation energies of both -1 and -2 charged peroxide species are negative. Therefore, the Gibbs free energy of these species should be more negative in solvents with greater static dielectric constant. Moreover, the rate of reduction in the Gibbs free energy of -2 charged peroxide is greater than that of the -1 charged peroxide ion due to its higher electrostatic charge.

The change in Gibbs free energy, which is the driving force for the multi-step reduction of oxygen into the peroxide ion, is obtained by adding the corresponding changes in free energies for the constituent reactions. Once the Gibbs free energies of all chemical species involved in each step were obtained from the DFT calculations, the change in Gibbs free energy of each reduction reaction was calculated in various ionic liquid electrolytes using eqn (7) and (8). These energies are shown in Fig. 7 as a function of the dielectric constant of the medium. The results presented in Fig. 7 show that the reduction of neutral oxygen into superoxide and superoxide into the peroxide ion in the vicinity of the carbon cathode are exothermic reactions. Furthermore, the change in Gibbs free energies of the reactions is more negative in ionic liquids with greater dielectric constant. In other words, the magnitude of the driving force for these reductions increases with increase in the static dielectric constant of the solvent medium.

The first reaction, which involves the reduction of oxygen into the superoxide ion, is exothermic. This is due in part to the positive electron affinity (EA) of oxygen, which results from its high electronegativity, as well as due to the negative solvation energy of oxygen and the superoxide ion. The theoretical electron affinity of a molecule, denotes the difference between the total energies of the neutral molecule and the anion at their respective optimized structures:⁵⁶

$$EA = E(A|A) - E(A^-|A^-) \quad (16)$$

Therefore, the electron affinity is positive for molecules in which the negatively charged anion lies energetically below the neutral molecule. Using the gas phase free energy of the oxygen molecule and the superoxide ion in their optimized structures, the electron affinity of the oxygen molecule was found to be 0.62 eV , which agrees closely with values reported in the literature.⁵⁶ While the addition of an extra electron to the negatively charged superoxide ion seems to be more difficult than the first reduction reaction, which is indeed true in the gas phase, the reduction of superoxide into the peroxide ion is still an exothermic reaction due to the large negative solvation free energy of the peroxide ion. The difference between the lowest

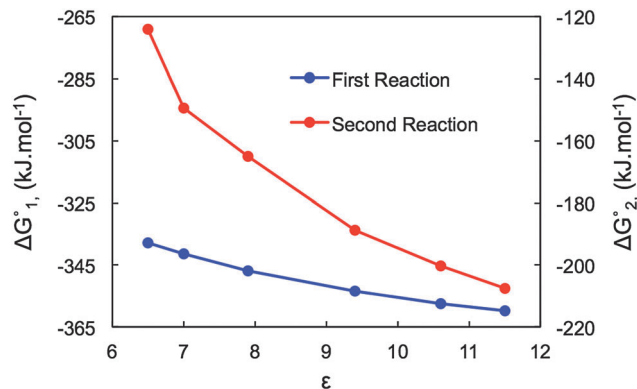


Fig. 7 The variation of the Gibbs free energy of both reduction reactions as a function of the static dielectric constant of the ionic liquids with varying alkyl side chain is shown.

and highest free energies of the first reaction in different ionic liquids is 22 kJ mol^{-1} while that for the second reaction is 83 kJ mol^{-1} . Therefore, the solvent medium has a stronger effect on the Gibbs free energy of the second reaction compared to that of the first reaction. This trend is expected since both the reactant and product species are charged particles in the second reaction unlike the first reaction, where neutral oxygen is the reactant species and is almost completely insensitive to the dielectric properties of the solvent medium.

The total reorganization energy, which is a required input to Marcus theory for calculating the electron transfer rate constant, was calculated for the reduction reactions described in eqn (1) and (2). The reorganization energies were calculated as the sum of inner-sphere reorganization energies, calculated using eqn (10) through (11), and the outer-sphere reorganization energies calculated using eqn (12). Fig. 8 shows the total reorganization energy for both reduction reactions in the forward and backward directions in ionic liquids with varying dielectric constants. The results presented in this figure indicate that the reorganization energy of both reduction reactions in both directions increases with increase in the dielectric constant.

The electronic coupling energy is an important parameter that is required for calculating the reaction rate for electron transfer in the framework of Marcus theory. The electronic coupling energies of the reduction reactions in each direction were calculated by employing the Corresponding Orbital Transformation method^{47,48} and are presented in Table 1. Based on this model, the electronic energies of reactants and products, the reactant-product overlap and the total interaction energies are calculated in the absence of external potential energy field such as the one created by the electrostatic field of solvent molecules. Therefore, the presence of solvent does not affect the electronic coupling energy.

Presented in Fig. 9 are the electron transfer rate constants for both reduction reactions in the forward and backward directions, in ionic liquids with varying static dielectric constants, which were evaluated in the framework of Marcus theory. Each data point corresponds to the reaction rate constant in the imidazolium based ionic liquids with a specific size of the alkyl side chain as shown in Fig. 3. The presented results

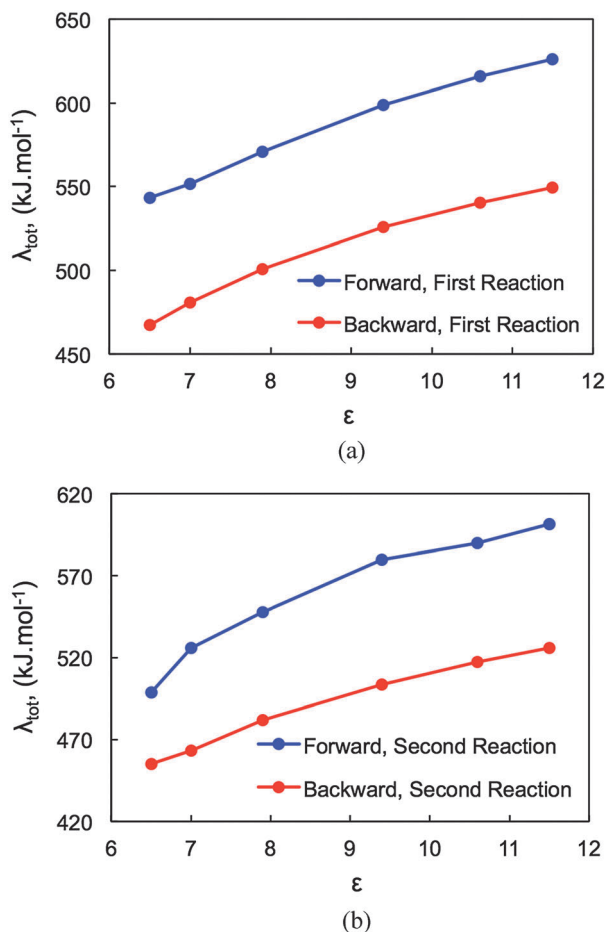


Fig. 8 The reorganization energy of (a) the reduction of oxygen into superoxide and (b) the reduction of superoxide into the peroxide ion in both forward and backward directions are shown as a function of the static dielectric constant of the solvent. The backward reactions correspond to the oxidation of superoxide and peroxide ions respectively.

show that the rate constants of the first reduction reaction in both directions and that of the second reaction in the backward direction decrease with increase in the static dielectric constant of the imidazolium based ionic liquid. The electron transfer rate constant of the second reduction reaction in the forward direction, however, remains almost constant with varying static dielectric constant. In this case, the maximum variation in the logarithm of the electron transfer rate constant in different ionic liquids is 0.98, which is only 7.4% of its average value. The very small values of the rate constants for the reverse reactions along with their positive Gibbs free energy change ($-\Delta G_1^\circ$ and $-\Delta G_2^\circ$) imply that these reactions are kinetically and thermodynamically unfavorable during the discharge cycle of the battery.

Table 1 Electronic coupling energies of the reduction reactions in both forward and backward directions

Reaction	V_{RP} of forward direction (J mol ⁻¹)	V_{RP} of backward direction (J mol ⁻¹)
$O_2 + e^- \rightleftharpoons O_2^-$	0.329	0.00551
$O_2 + e^- \rightleftharpoons O_2^{2-}$	0.00394	0.000525

Since the electron transfer reaction in each reduction step is considered as an elementary reaction, the equilibrium constant of each step can be calculated using the ratio of the corresponding forward and backward rate constants:

$$K_{eq,1} = \frac{k_1}{k_{-1}} \quad (17)$$

$$K_{eq,2} = \frac{k_2}{k_{-2}} \quad (18)$$

where, $K_{eq,1}$ and $K_{eq,2}$ are the equilibrium constants for the reduction of oxygen and superoxide respectively. k_1 , k_{-1} and k_2 , k_{-2} are the forward and backward rate constants of the first and second reduction reactions respectively. Given the Gibbs free energy of each reduction reaction, the electron transfer rate constant of the backward reactions can be calculated using the following set of equations:

$$k_{-1} = k_1 \exp\left(\frac{\Delta G_1^\circ}{RT}\right) \quad (19)$$

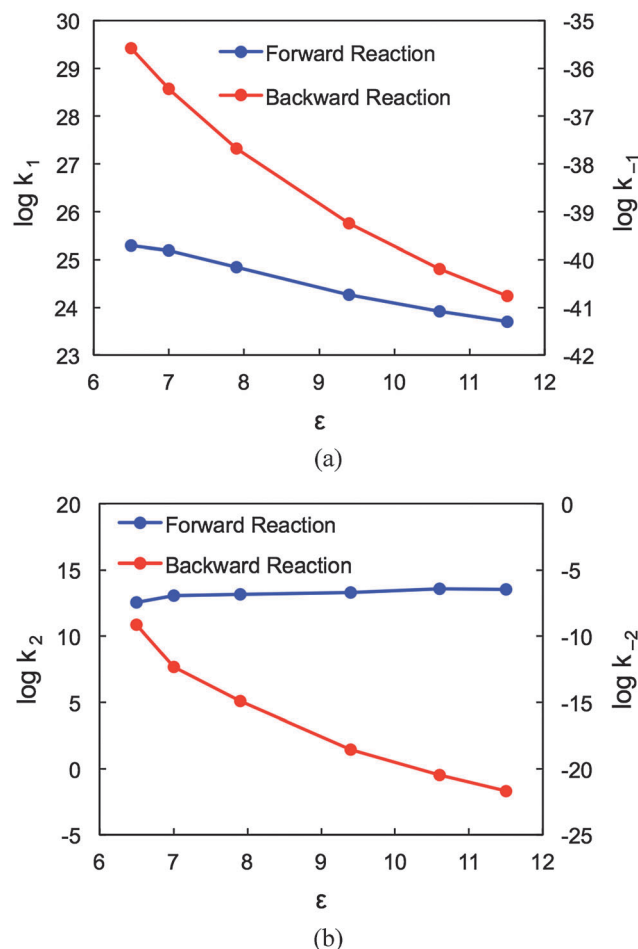


Fig. 9 The electron transfer rate constant of (a) the reduction of oxygen into superoxide and (b) the reduction of superoxide into the peroxide ion in both forward and backward directions in imidazolium based ionic liquids with varying static dielectric constant is shown. The backward reactions correspond to the oxidation of superoxide and peroxide ions respectively.

$$k_{-2} = k_2 \exp\left(\frac{\Delta G_2^\circ}{RT}\right) \quad (20)$$

The calculated electron transfer rate constants for the backward reactions, using this indirect method, are slightly different from those calculated using Marcus theory. The average relative errors in calculating the backward electron transfer rate constants using the indirect method are 4.3% and 4.9% for the first and second reduction reactions respectively. These errors result from the accumulated errors in calculating the reorganization and electronic coupling energies that are used in Marcus theory.

The overall rate constant of the reduction of oxygen into the peroxide ion was calculated using a method that is described in the ESI.† The overall rate constant, presented in Fig. 10, shows the same trend as the forward rate constant of the first reduction step. This figure shows that the electron transfer rate constant, in a logarithmic scale, is nearly proportional to the inverse of the static dielectric constant of the solvent. Consequently, decreasing the static dielectric constant of the solvent increases the electron transfer reaction rate. Therefore, in imidazolium based ionic liquids containing TFSI⁻ as the anion, the electron transfer reaction at the cathode occurs faster in ionic liquids that have cations with longer alkyl side chains. As shown in Fig. 10, the fitted expression for the variation of the rate constant with the dielectric constant is given as: $\log k_{\text{et}}(\text{tot}) = 24.598(1/\epsilon) + 21.62$. The dielectric constant is the most important solvent parameter affecting the rate constant for electron transfer. The fitted expression can be further beneficial in determining an approximate value of the rate constant for the reduction of oxygen in other ionic liquids that comprise the TFSI⁻ anion and have a dielectric constant that vary within the studied range.

Realistic operating temperatures in lithium batteries range from $-15\text{ }^\circ\text{C}$ to $100\text{ }^\circ\text{C}$. In order to investigate the effect of temperature on the electron transfer reaction rate constants, all the above-mentioned thermodynamic parameters were calculated in a temperature range from $-15\text{ }^\circ\text{C}$ to $100\text{ }^\circ\text{C}$ in $[\text{C}_2\text{MIM}]^+[\text{TFSI}]^-$ as the solvent and the corresponding rate constants for each reduction reaction in both forward and backward directions were calculated. The results presented in Fig. 11 show that with increase in the temperature, the Gibbs free energies of all species have negative values of increasingly greater magnitude.

Using the calculated Gibbs free energies of the optimized oxygen molecule, superoxide and peroxide structures with varying charges, the change in Gibbs free energies for the reduction of oxygen into superoxide and the reduction of superoxide to the peroxide ion was calculated in the studied temperature range. Fig. 12 shows the variation of the Gibbs free energies of these two reduction reactions with temperature. The Gibbs free energy for both reactions increases in magnitude with increasing temperature. However, the change in the Gibbs free energy for the reduction of superoxide into the peroxide ion is more significant than that of the reduction of oxygen. This effect is due to the higher entropy change for the second reduction reaction. At constant pressure, the negative of the first derivative of Gibbs free energy with respect to temperature, $-\left(\frac{\partial \Delta G^\circ}{\partial T}\right)_P$, which is the slope of the change in the

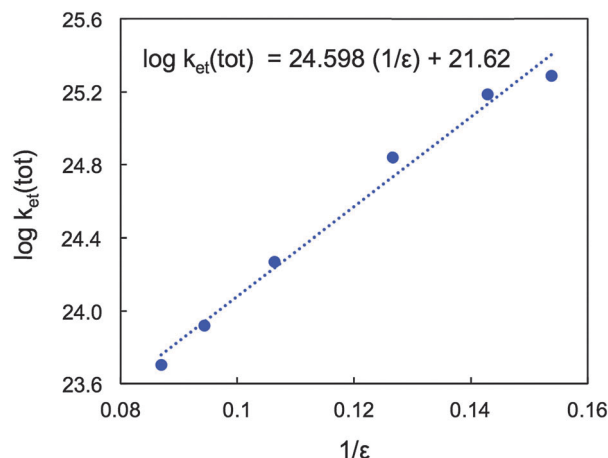


Fig. 10 Variation of the overall rate constant for the reduction of oxygen into the peroxide ion due to electron transfer is shown as a function of the static dielectric constant of the solvent.

Gibbs free energy of the reaction with temperature, is equal to the entropy change of the reaction at each temperature, ΔS_T :

$$\Delta S_T = -\left(\frac{\partial \Delta G^\circ}{\partial T}\right)_P \quad (21)$$

Therefore, the magnitude of the slope of the fitted linear expressions is equal to the average entropy change of each reduction reaction. The average entropy change of the first and second reduction reactions is 0.002 and $0.0039\text{ kJ mol}^{-1}\text{ K}^{-1}$ respectively, which are equal to the magnitude of the slope of the corresponding fitted lines shown in Fig. 12.

Furthermore, the Gibbs free energy of each species provided in Fig. 11 was used to evaluate the reorganization energies of both reactions in forward and backward directions as a function of temperature. We assumed that the outer-sphere reorganization energy is independent of temperature. The results presented in Fig. 13 show that with increase in the temperature, the reorganization energy of forward reactions increases. For the backward reactions, however, the reorganization energy decreases with increasing temperature.

The electron transfer rate constant of the reduction reactions in forward and backward directions was evaluated using the calculated thermodynamic parameters at varying temperature. The results, presented in Fig. 14, show that the electron transfer rate constants for both reduction reactions in both directions increase with increasing temperature. However, as shown in Fig. 14(a), for the reduction of oxygen into superoxide, the rate of increase for the backward rate constant is greater than that of the forward rate constant. According to eqn (19):

$$\ln K_{\text{eq},1} = -\frac{\Delta G_1^\circ}{RT} \quad (22)$$

By taking the derivative of both sides with respect to temperature at constant pressure we get:

$$\frac{d \ln K_{\text{eq},1}}{dT} = \frac{\Delta G_1^\circ}{RT^2} - \frac{1}{RT} \left(\frac{\partial \Delta G_1^\circ}{\partial T}\right)_P \quad (23)$$

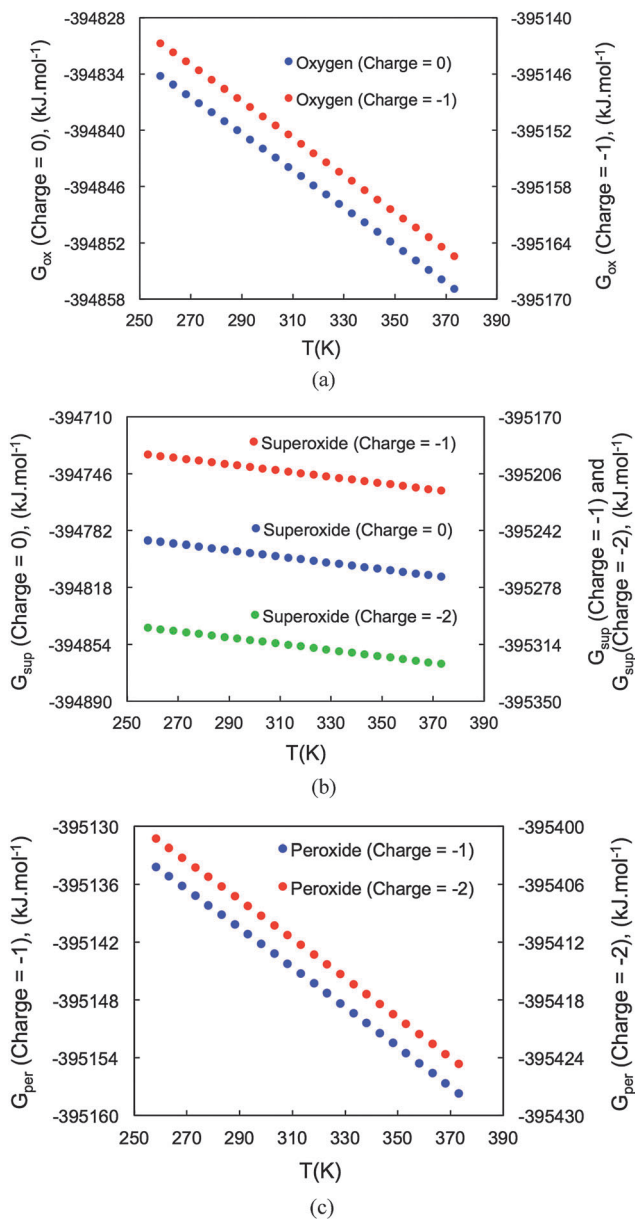


Fig. 11 The variations of the Gibbs free energy of (a) neutral and $-1 e$ charged oxygen molecule, (b) neutral, -1 and -2 charged superoxide structures and (c) -1 and -2 charged peroxide structures at various operating temperatures are presented. The nomenclature G_{ox} , G_{sup} and G_{per} indicate that the optimized structures used in calculating the Gibbs free energies correspond to that of the standard oxygen molecule, superoxide ion and peroxide ion respectively.

Moreover, we know that $\left(\frac{\partial \Delta G_1^\circ}{\partial T}\right)_p = -\Delta S_1^\circ$. Hence:

$$\frac{d \ln K_{eq,1}}{dT} = \frac{\Delta G_1^\circ}{RT^2} + \frac{\Delta S_1^\circ}{RT} = \frac{\Delta G_1^\circ + T\Delta S_1^\circ}{RT^2} = \frac{\Delta H_1^\circ}{RT^2} \quad (24)$$

The maximum difference in ΔH_1° in the studied temperature range is $0.09714 \text{ kJ mol}^{-1}$, which is merely 0.027% of the average value. Therefore, we can assume that ΔH_1° is constant in this temperature range. Hence if we integrate both sides:

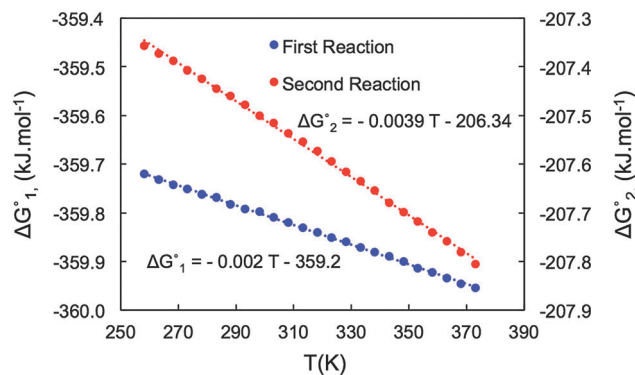


Fig. 12 Variation of the Gibbs free energies of reduction of oxygen and the superoxide ion at various temperatures. The effect of temperature is more prominent for the second step involving the reduction of the superoxide ion to peroxide, based on the fitted slopes.

$$\ln \frac{K_{eq,1}(T_2)}{K_{eq,1}(T_1)} = -\frac{\Delta H_1^\circ}{R} \left(\frac{1}{T_2} - \frac{1}{T_1} \right) \quad (25)$$

Since ΔH° for the first reduction reaction is negative, with an average value of $-359.196 \text{ kJ mol}^{-1}$, the equilibrium constant for the reaction decreases with increasing temperature. Moreover, based on eqn (17), the equilibrium constant for this reaction is the ratio of the forward to the backward rate

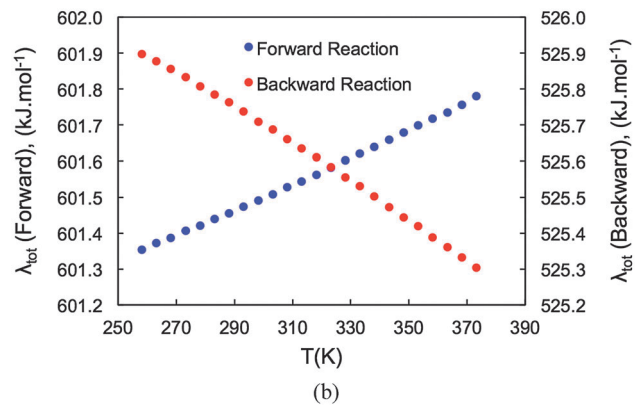
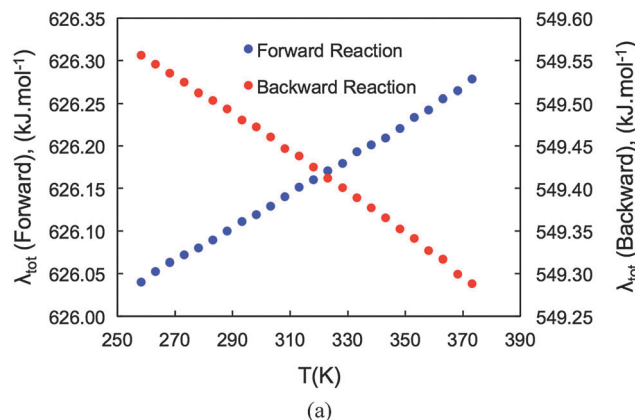
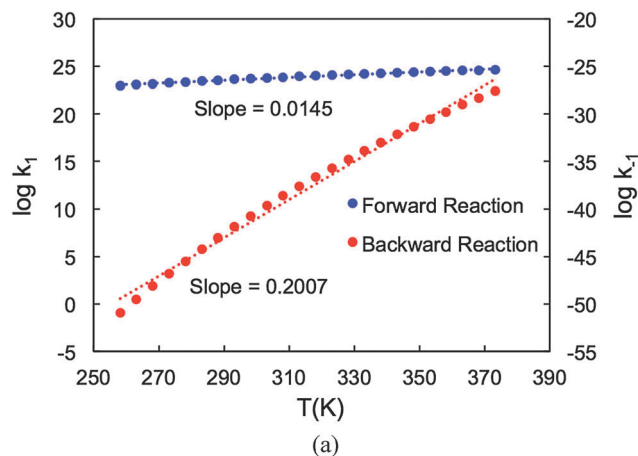
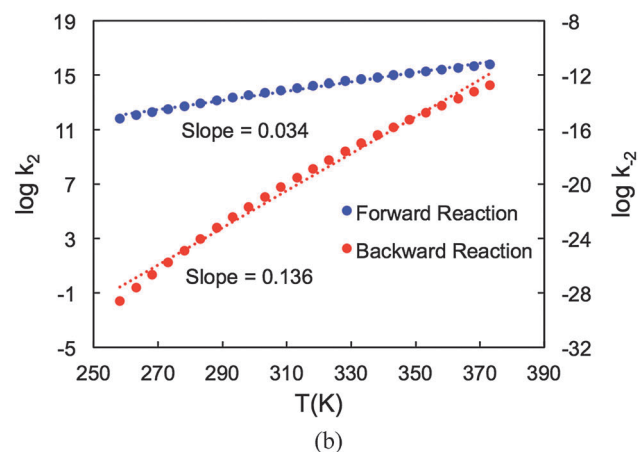


Fig. 13 The variation of the total reorganization energies of (a) the reduction of oxygen and (b) superoxide in both forward and backward directions are shown at various temperatures.



(a)



(b)

Fig. 14 The variation of the rate constant of (a) reduction of oxygen into superoxide and (b) reduction of superoxide into peroxide with temperature is shown. In both reduction reactions the rate of increase for the forward rate constant is smaller than that of the backward rate constant.

constant for the reaction. Therefore, since both forward and backward rate constants of the reaction increase with increasing temperature, the rate of increase for the backward rate constant should be greater than that of the forward rate constant in order to maintain the decrease in the equilibrium constant. The change in enthalpy, ΔH° , for the reduction of superoxide into peroxide is also negative with an average value of $-206.328 \text{ kJ mol}^{-1}$ and a maximum difference of only 0.153% of the average. So, the above equations and assumptions will be valid for the second reaction as well. Therefore, as shown in Fig. 14(b), for the reduction of superoxide into the peroxide ion, the rate of increase for the forward rate constant is smaller than that of the backward rate constant.

Ultimately, the overall rate constant of the reduction of oxygen into the peroxide ion is calculated in the studied temperature range from $-15 \text{ }^\circ\text{C}$ to $100 \text{ }^\circ\text{C}$. The results are presented in Fig. 15 and indicate that the electron transfer rate constant on the logarithmic scale is directly proportional to the inverse of the operating temperature. Therefore, it is concluded that in imidazolium based ionic liquids with TFSI^- as the anion, the electron transfer reaction at the cathode happens faster at higher operating temperatures.

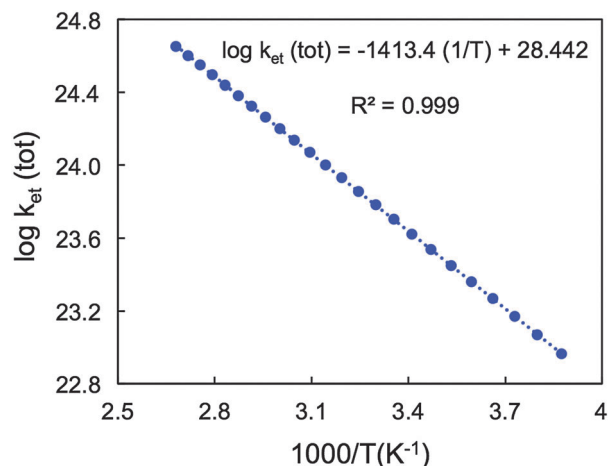


Fig. 15 The variation of the overall rate constant of the reduction of oxygen into the peroxide ion with the inverse of operating temperature is shown.

Conclusions

In this study, the kinetics of the multi-step electrochemical reduction of oxygen at the carbon based cathode of the Li-air battery was investigated. The reaction rate constants for electron transfer from the graphite cathode to the oxygen molecule and the superoxide ion as well as the reverse reactions were calculated in ionic liquid electrolytes with varying dielectric constants and at various operating temperatures using density functional theory (DFT). Marcus theory formulation was applied to evaluate the rate constant, and the effect of solvent on these reaction rates was investigated using the COSMO solvation model. We calculated the Gibbs free energy for the individual steps involved in the reduction of oxygen into the peroxide ion. Our calculations indicate that by decreasing the dielectric constant of the solvent, which is a consequence of increasing the number of carbon atoms in the alkyl side chain of the cation, the magnitude of the Gibbs free energy of the reduction of oxygen into the superoxide ion as well as that of the reduction of superoxide into the peroxide ion, decreases. Moreover, the Gibbs free energy of these two reduction reactions increases in magnitude with increase in the operating temperature of the Li-air battery. We also evaluated the inner-sphere and outer-sphere reorganization energies associated with the electron transfer reactions at the cathode in the presence of various ionic liquid solvents. Our results indicate that the total reorganization energies associated with the electron transfer reduction of the oxygen molecule and the superoxide ion increase with the increase in the static dielectric constant of the solvent as well as with increase in the operating temperature. The calculated Gibbs free energy, total reorganization energy and coupling energy values were used to calculate the reaction rate constant in the framework of Marcus theory. The results demonstrate that a decrease in the static dielectric constant of the ionic liquid electrolyte, due to an increase in the length of the alkyl side chain of the imidazolium cation, results in an increase in the reaction rate constant for reduction of the

oxygen molecule into the peroxide ion involving electron transfer at the cathode. The increase in the logarithm of the electron transfer rate constant shows a linear trend with respect to the inverse of the static dielectric constant of the ionic liquid medium. Moreover, the overall reaction rate constant for the reduction of oxygen into the peroxide ion increases with increase in the operating temperature. The fitted mathematical relation can be extended to evaluate the rate constant of the reduction of oxygen in ionic liquids with the TFSI⁻ anion if the dielectric constant of the ionic liquid, and the operating temperature vary within the studied range.

Funding sources

This project was funded by the Joint Center for Aerospace Technology Innovation (JCATI) sponsored by the State of Washington.

Acknowledgements

The authors acknowledge the use of Washington State University's high performance computing cluster for carrying out the simulations. The authors acknowledge funding from the Joint Center for Aerospace Technology Innovation (JCATI) sponsored by the State of Washington.

References

- G. Girishkumar, B. McCloskey, A. C. Luntz, S. Swanson and W. Wilcke, Lithium – Air Battery: Promise and Challenges, *J. Phys. Chem. Lett.*, 2010, **1**, 2193–2203.
- J. Christensen, P. Albertus, R. S. Sanchez-Carrera, T. Lohmann, B. Kozinsky, R. Liedtke, J. Ahmed and A. Kojic, A Critical Review of Li/Air Batteries, *J. Electrochem. Soc.*, 2012, **159**, R1–R30.
- M. A. Rahman, X. Wang and C. Wen, A Review of High Energy Density Lithium-Air Battery Technology, *J. Appl. Electrochem.*, 2014, **44**, 5–22.
- N. Imanishi and O. Yamamoto, Rechargeable Lithium-Air Batteries: Characteristics and Prospects., *Mater. Today*, 2014, **17**, 24–30.
- C. W. Kamienski, D. P. McDonald, M. W. Stark and J. R. Papcun, *Lithium and Lithium Compounds*, John Wiley & Sons, Inc., 2004.
- A. K. Furr, *CRC Handbook of Laboratory Safety*, CRC Press, Boca Raton, 2000.
- E. P. Roth and C. J. Orendorff, How Electrolytes Influence Battery Safety, *Electrochem. Soc. Interface*, 2012, **21**, 45–49.
- G.-A. Nazri and G. Pistoia, *Lithium Batteries: Science and Technology*, Springer, Boston, 2003, pp. 610–611.
- R. A. Marsh, S. Vukson, S. Surampudi, B. V. Ratnakumar, M. C. Smart, M. Manzo and P. J. Dalton, Li Ion Batteries for Aerospace Applications, *J. Power Sources*, 2001, **97**, 25–27.
- A. Lewandowski and A. Swiderska-Mocek, Ionic Liquids As Electrolytes for Li-Ion Batteries-An Overview of Electrochemical Studies, *J. Power Sources*, 2009, **194**, 601–609.
- M. Galinski, A. Lewandowski and I. Stepniak, Ionic Liquids As Electrolytes, *Electrochim. Acta*, 2006, **51**, 5567–5580.
- A. Deshpande, L. Kariyawasam, P. Dutta and S. Banerjee, Enhancement of Lithium Ion Mobility in Ionic Liquid Electrolytes in Presence of Additives, *J. Phys. Chem. C*, 2013, **117**, 25343–25351.
- N. V. Plechkova and K. R. Seddon, Applications of Ionic Liquids in the Chemical Industry, *Chem. Soc. Rev.*, 2008, **37**, 123–150.
- J. S. Newman, *Electrochemical Systems*, 3rd edn, Englewood Cliffs, NJ, 1972.
- K. Yoo, S. Banerjee and P. Dutta, Modeling of Volume Change Phenomena in a Li-Air Battery, *J. Power Sources*, 2014, **258**, 340–350.
- J. S. Hummelshoj, J. Blomqvist, S. Datta, T. Vegge, J. Rossmeisl, K. S. Thygesen, A. C. Luntz, K. W. Jacobsen and J. K. Nørskov, Communications: Elementary Oxygen Electrode Reactions in the Aprotic Li-Air Battery, *J. Chem. Phys.*, 2010, **132**, 071101.
- X. Ren, S. S. Zhang, D. T. Tran and J. Read, Oxygen Reduction Reaction Catalyst on Lithium/Air Battery Discharge Performance, *J. Mater. Chem.*, 2011, **21**, 10118–10125.
- C. O. Laoire, S. Mukerjee, K. M. Abraham, E. J. Plichta and M. A. Hendrickson, Elucidating the Mechanism of Oxygen Reduction for Lithium-Air Battery Applications, *J. Phys. Chem. C*, 2009, **113**, 20127–20134.
- N. Seriani, Ab Initio Thermodynamics of Lithium Oxides: From Bulk Phases to Nanoparticles, *Nanotechnology*, 2009, **20**, 445703.
- V. S. Bryantsev, M. Blanco and F. Faglioni, Stability of Lithium Superoxide LiO₂ in the Gas Phase: Computational Study of Dimerization and Disproportionation Reactions, *J. Phys. Chem. A*, 2010, **114**, 8165–8169.
- K. M. Abraham and Z. Jiang, A Polymer Electrolyte-Based Rechargeable Lithium/Oxygen Battery, *J. Electrochem. Soc.*, 1996, **143**, 1–5.
- J. Read, Characterization of the Lithium/Oxygen Organic Electrolyte Battery, *J. Electrochem. Soc.*, 2002, **149**, A1190–A1195.
- S. Kazemiabnavi, P. Dutta and S. Banerjee, Density Functional Theory Based Study of the Electron Transfer Reaction at the Lithium Metal Anode in a Lithium-Air Battery with Ionic Liquid Electrolytes, *J. Phys. Chem. C*, 2014, **118**, 27183–27192.
- S. Kazemiabnavi, P. Dutta and S. Banerjee, Ab Initio Modeling of the Electron Transfer Reaction Rate at the Electrode-Electrolyte Interface in Lithium-Air Batteries, *ASME 2014 IMECE*, American Society of Mechanical Engineers, Montreal, Canada, 2014, Vol. 6A: Energy, doi: 10.1115/IMECE2014-40239.
- T. Singh and A. Kumar, Static Dielectric Constant of Room Temperature Ionic Liquids: Internal Pressure and Cohesive Energy Density Approach, *J. Phys. Chem. B*, 2008, **112**, 12968–12972.
- S. P. Ong, O. Andreussi, Y. Wu, N. Marzari and G. Ceder, Electrochemical Windows of Room-Temperature Ionic Liquids from Molecular Dynamics and Density Functional Theory Calculations, *Chem. Mater.*, 2011, **23**, 2979–2986.
- S. Sowmiah, V. Srinivasadesikan, M.-C. Tseng and Y.-H. Chu, On the Chemical Stabilities of Ionic Liquids, *Molecules*, 2009, **14**, 3780–3813.

- 28 S. Zhang, N. Sun, X. He, X. Lu and X. Zhang, Physical Properties of Ionic Liquids: Database and Evaluation, *J. Phys. Chem. Ref. Data*, 2006, **35**, 1475–1517.
- 29 M.-M. Huang, Y. Jiang, P. Sasisanker, G. W. Driver and H. Weingartner, Static Relative Dielectric Permittivities of Ionic Liquids at 25 °C, *J. Chem. Eng. Data*, 2011, **56**, 1494–1499.
- 30 P. Bonhote, A. P. Dias, N. Papageorgiou, K. Kalyanasundaram and M. Gratzel, Hydrophobic, Highly Conductive Ambient-Temperature Molten Salts, *Inorg. Chem.*, 1996, **35**, 1168–1178.
- 31 E. Gomez, N. Calvar, E. A. Macedo and A. Dominguez, Effect of the Temperature on the Physical Properties of Pure 1-Propyl 3-Methylimidazolium Bis(trifluoromethylsulfonyl)imide and Characterization of its Binary Mixtures with Alcohols, *J. Chem. Thermodyn.*, 2012, **45**, 9–15.
- 32 H. Olivier-Bourbigou and L. Magna, Ionic Liquids: Perspectives for Organic and Catalytic Reactions, *J. Mol. Catal. A: Chem.*, 2002, **182**, 419–437.
- 33 K. R. Harris, M. Kanakubo and L. A. Woolf, Temperature and Pressure Dependence of the Viscosity of the Ionic Liquid 1-Butyl-3-Methylimidazolium Tetrafluoroborate: Viscosity and Density Relationships in Ionic Liquids, *J. Chem. Eng. Data*, 2007, **52**, 2425–2430.
- 34 K. R. Harris, M. Kanakubo and L. A. Woolf, Temperature and Pressure Dependence of the Viscosity of the Ionic Liquids 1-Hexyl-3-Methylimidazolium Hexafluorophosphate and 1-Butyl-3-Methylimidazolium Bis(trifluoromethylsulfonyl)imide, *J. Chem. Eng. Data*, 2007, **52**, 1080–1085.
- 35 R. G. de Azevedo, J. Esperanca, J. Szydowski, Z. P. Visak, P. F. Pires, H. J. R. Guedes and L. P. N. Rebelo, Thermophysical and Thermodynamic Properties of Ionic Liquids Over an Extended Pressure Range: BMIM NTf₂ and HMIM NTf₂, *J. Chem. Thermodyn.*, 2005, **37**, 888–899.
- 36 S. Carda-Broch, A. Berthod and D. W. Armstrong, Solvent Properties of the 1-Butyl-3-Methylimidazolium Hexafluorophosphate Ionic Liquid, *Anal. Bioanal. Chem.*, 2003, **375**, 191–199.
- 37 C. Schreiner, S. Zugmann, R. Hartl and H. J. Gores, Fractional Walden Rule for Ionic Liquids: Examples from Recent Measurements and a Critique of the So-Called Ideal KCl Line for the Walden Plot, *J. Chem. Eng. Data*, 2010, **55**, 1784–1788.
- 38 C. Schreiner, S. Zugmann, R. Hartl and H. J. Gores, Temperature Dependence of Viscosity and Specific Conductivity of Fluoroborate-Based Ionic Liquids in Light of the Fractional Walden Rule and Angell's Fragility Concept, *J. Chem. Eng. Data*, 2010, **55**, 4372–4377.
- 39 D. G. Truhlar, B. C. Garrett and S. J. Klippenstein, Current Status of Transition-State Theory, *J. Phys. Chem.*, 1996, **100**, 12771–12800.
- 40 D. G. Truhlar and B. C. Garrett, Variational Transition-State Theory, *Annu. Rev. Phys. Chem.*, 1984, **35**, 159–189.
- 41 Y. Wang, Y. Qian, W. L. Feng and R. Z. Liu, Implementation of a Microcanonical Variational Transition State Theory for Direct Dynamics Calculations of Rate Constants, *Sci. China, Ser. B: Chem.*, 2003, **46**, 225–233.
- 42 B. C. Garrett and D. G. Truhlar, Generalized Transition State Theory. Canonical Variational Calculations Using the Bond Energy-Bond Order Method for Bimolecular Reactions of Combustion Products, *J. Am. Chem. Soc.*, 1979, **101**, 5207–5217.
- 43 R. A. Marcus, Electron Transfer Reactions in Chemistry. Theory and Experiment, *Pure Appl. Chem.*, 1997, **69**, 13–29.
- 44 S. F. Nelsen, S. C. Blackstock and Y. Kim, Estimation of Inner Shell Marcus Terms for Amino Nitrogen Compounds by Molecular Orbital Calculations, *J. Am. Chem. Soc.*, 1987, **109**, 677–682.
- 45 Q. Wu and T. Van Voorhis, Direct Calculation of Electron Transfer Parameters Through Constrained Density Functional Theory, *J. Phys. Chem. A*, 2006, **110**, 9212–9218.
- 46 D. C. Sorescu, K. D. Jordan and P. Avouris, Theoretical Study of Oxygen Adsorption on Graphite and The (8,0) Single-Walled Carbon Nanotube, *J. Phys. Chem. B*, 2001, **105**, 11227–11232.
- 47 A. Farazdel, M. Dupuis, E. Clementi and A. Aviram, Electric-Field Induced Intramolecular Electron-transfer in Spiro Pi-Electron Systems and Their Suitability as Molecular Electronic Devices – A Theoretical-Study, *J. Am. Chem. Soc.*, 1990, **112**, 4206–4214.
- 48 N. Koga, K. Sameshima and K. Morokuma, Ab-initio MO Calculations of Electronic Coupling Matrix-Element on Model Systems for Intramolecular Electron-Transfer, Hole Transfer and Triplet Energy-Transfer – Distance Dependence and Pathway in Electron-Transfer and Relationship of Triplet Energy-Transfer with Electron and Hole Transfer, *J. Phys. Chem.*, 1993, **97**, 13117–13125.
- 49 A. D. Becke, Density-Functional Thermochemistry.3. The Role of Exact Exchange, *J. Chem. Phys.*, 1993, **98**, 5648–5652.
- 50 C. T. Lee, W. T. Yang and R. G. Parr, Development of the Colle-Salvetti Correlation-Energy Formula into a Functional of the Electron-Density, *Phys. Rev. B: Condens. Matter Mater. Phys.*, 1988, **37**, 785–789.
- 51 R. Krishnan, J. S. Binkley, R. Seeger and J. A. Pople, Self-Consistent Molecular-Orbital Methods.20. Basis Set for Correlated Wave-Functions, *J. Chem. Phys.*, 1980, **72**, 650–654.
- 52 M. Valiev, E. J. Bylaska, N. Govind, K. Kowalski, T. P. Straatsma, H. J. J. Van Dam, D. Wang, J. Nieplocha, E. Apra, T. L. Windus and W. de Jong, NWChem: A Comprehensive and Scalable Open-Source Solution for Large Scale Molecular Simulations, *Comput. Phys. Commun.*, 2010, **181**, 1477–1489.
- 53 A. Klamt and G. Schuurmann, COSMO – A New Approach to Dielectric Screening in Solvents with Explicit Expressions for the Screening Energy and its Gradient, *J. Chem. Soc., Perkin Trans. 2*, 1993, 799–805.
- 54 M. N. Kobrak, The Relationship Between Solvent Polarity and Molar Volume in Room-Temperature Ionic Liquids, *Green Chem.*, 2008, **10**, 80–86.
- 55 H. Tjong and H.-X. Zhou, GBr(6): A Parameterization-Free, Accurate, Analytical Generalized Born Method, *J. Phys. Chem. B*, 2007, **111**, 3055–3061.
- 56 J. C. Rienstra-Kiracofe, G. S. Tschumper, H. F. Schaefer, S. Nandi and G. B. Ellison, Atomic and Molecular Electron Affinities: Photoelectron Experiments and Theoretical Computations, *Chem. Rev.*, 2002, **102**, 231–282.